angles the effect on the thermal parameters may be appreciable.

On some occasions the polarization ratio K has been included in the parameters that are refined. The results have not been encouraging as the values may have fallen far outside the bounds of direct determinations (Vincent & Flack, 1980; Bachmann, Kohler, Schulz & Weber, 1984). This is not very surprising in the light of the above findings, which demonstrate that a smooth angular function can be absorbed in the model in many different ways.

The users of diffractometers are urged to determine K experimentally, or at least to make an estimate as outlined in the *Introduction*. The values given in Table 1 suggest that the dynamical value for K is a better estimate than the customarily used kinematical value. Jennings (1984) lists 40 determinations of K in a survey conducted for the International Union of Crystallography Commission on Crystallographic Apparatus. These results also give guidelines for an estimation of K.

The financial support by the Academy of Finland of one of the authors (PS) is gratefully acknowledged.

References

BACHMANN, R., KOHLER, H., SCHULZ, H. & WEBER, H.-P. (1984). *Acta Cryst.* A**40**, C400.
BECKER, P. J. & COPPENS, P. (1974). *Acta Cryst.* A**30**, 129-147.
JAMES, R. W. (1962). *The Optical Principles of the Diffraction of X-rays*. London: G. Bell and Sons.
JENNINGS, L. D. (1981). *Acta Cryst.* A**37**, 584-593.
JENNINGS, L. D. (1984). *Acta Cryst.* A**40**, 12-16.
LE PAGE, Y., GABE, E. J. & CALVERT, L. D. (1979). *J. Appl. Cryst.* **12**, 25-26.
MATERLIK, G. & SUORTTI, P. (1984). *J. Appl. Cryst.* **17**, 7-12.
OLEKHNOVICH, N. M. (1969). *Sov. Phys. Crystallogr.* **14**, 203-206.
OLEKHNOVICH, N. M., MARKOVICH, V. L., OLEKHNOVICH, A. N. & POLUCHANKINA, L. P. (1981). *Izv. Akad. Nauk BSSR*, No. 2, 64-67.
SUORTTI, P. & JENNINGS, L. D. (1977). *Acta Cryst.* A**33**, 1012-1027.
VINCENT, M. G. & FLACK, H. D. (1980). *Acta Cryst.* A**36**, 614-620.
ZACHARIASEN, W. H. (1945). *Theory of X-ray Diffraction in Crystals*. New York: John Wiley & Sons.

Acta Cryst. (1986). A**42**, 188-191

Neutron Diffraction from Single-Crystal Silicon: the Dependence of the Thermal Diffuse Scattering on the Velocity of Sound

BY B. T. M. WILLIS*

*AERE Harwell, Didcot, Oxon OX*11 0*RA, England*

AND C. J. CARLILE AND R. C. WARD

*Rutherford Appleton Laboratory, Chilton, Didcot, Oxon OX*11 0*QX, England*

(*Received* 20 *June* 1985; *accepted* 7 *November* 1985)

Abstract

It is well known [Willis (1970). *Acta Cryst.* A**26**, 396-401] from the theory of one-phonon scattering of thermal neutrons by a crystal that the nature of the thermal diffuse scattering (TDS) near the Bragg peak depends on whether the neutron velocity is greater than or is less than the sound velocity in the crystal. For faster-than-sound neutrons the TDS rises to a peak coinciding with the Bragg peak, whereas for slower-than-sound neutrons the TDS tends to give a flat background across the Bragg reflection. These theoretical predictions are supported by experiments using pulsed neutron diffraction from single crystals of perfect silicon. In particular, the integrated TDS across a reflection undergoes a pronounced fall when the neutron velocity drops below the velocity of sound.

* Now at: Chemical Crystallography Laboratory, 9 Parks Road, Oxford OX1 3PD, England.

0108-7673/86/030188-04$01.50

1. Introduction

In a diffraction experiment, with either a single crystal or a polycrystalline sample, the measured intensity of a Bragg reflection will include a contribution from thermal diffuse scattering (TDS) which arises from the scattering of the incident beam by phonons. For X-rays, the one-phonon TDS is not subtracted with the background measured on either side of the reflection, since it rises to a maximum at the same point as the Bragg peak itself. This then causes the so-called TDS error in estimating Bragg intensities.

For thermal neutrons, the situation is quite different (Willis, 1970). The reason is that the neutron energy is comparable with the phonon energy, whereas X-rays have energies that are five orders of magnitude higher. Consequently, the condition

$$|\mathbf{k}| = |\mathbf{k}_0| \qquad (1)$$

(where $\mathbf{k}$ and $\mathbf{k}_0$ are the wave vectors of the scattered

and incident radiation respectively) for the one-phonon scattering of X-rays does not apply to neutrons. Instead we must write

$$|\mathbf{k}| = |\mathbf{k}_0| - \varepsilon\beta q, \qquad (2)$$

where the extra term, $\varepsilon\beta q$, is comparable in magnitude with $|\mathbf{k}| - |\mathbf{k}_0|$. ε in (2) is either +1 or −1: $\varepsilon = +1$ corresponds to phonon emission (creation) and $\varepsilon = -1$ to phonon absorption (annihilation). β is the ratio of the velocity of sound in the crystal to the neutron velocity, and q is the wave number of the phonon associated with the scattering process. It is assumed in (2) that $q \ll k_0$ (*i.e.* that the TDS is close to the Bragg position) and that the velocity of sound associated with each acoustic mode is isotropic.

Before calculating the intensity of the TDS at a given setting of the crystal it is necessary to define the locus in reciprocal space of the end point of the phonon wave vector **q**. This locus is referred to as the scattering surface. [The phonon wave vector **q** joins the end points of the scattering vector $(\mathbf{k} - \mathbf{k}_0)$ and the reciprocal-lattice vector.] For X-rays this locus coincides with the Ewald sphere in accordance with (1), but for neutrons it is more complicated. From (2) the end point of **q** lies on a conic of eccentricity $1/\beta$.* If the neutrons are faster than sound ($\beta < 1$), the locus is a hyperboloid of two sheets, with the **q** vectors on one sheet corresponding to emission of phonons and on the other sheet to absorption. If the neutrons are slower than sound ($\beta > 1$), the locus is an ellipsoid: scattering now occurs either by emission or by absorption but not by both together. These two types of neutron scattering surface are illustrated in Fig. 1.

* This is strictly correct for $\theta = 0$ only. For $\theta > 0$, the eccentricity is $1/(\beta \cos\theta)$: see § 3 for the origin of this geometrical term.

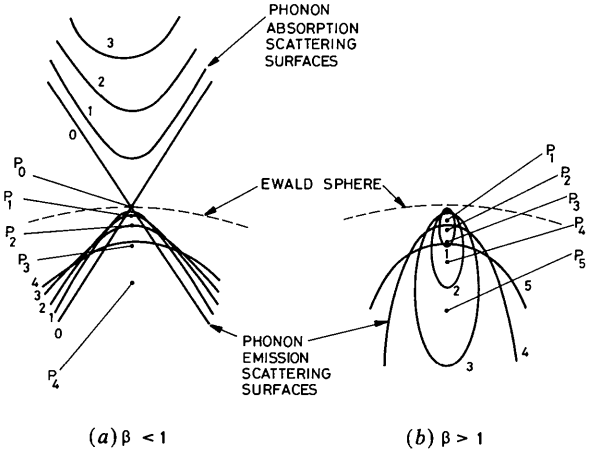

Fig. 1. Scattering surfaces for one-phonon scattering of neutrons: (*a*) for neutrons faster than sound, (*b*) for neutrons slower than sound. The scattering surface for X-rays is the Ewald sphere (broken lines). $P_0, P_1, \ldots, P_5$ are different positions of the reciprocal-lattice point with respect to the Ewald sphere (after Cooper, 1971).

Knowing the geometry of the scattering surface for each setting of the crystal, and applying standard formulae for the one-phonon scattering cross section associated with each **q** vector lying on the surface, we can calculate easily the integrated TDS intensity, I_{TDS}, lying above the straight-line background across the Bragg peak. The results are (Cooper, 1971):

(*a*) X-rays. The TDS rises to a maximum at the Bragg peak and the TDS error can be derived if the elastic constants of the crystal are known.

(*b*) Neutrons: $\beta < 1$. The TDS rises to a maximum, just as for X-rays, and I_{TDS} is obtained using the same formulae as for X-rays with the scattering factor for X-rays replaced by the neutron scattering amplitude. [This is a remarkable result in view of the different scattering surfaces for (*a*) and (*b*).]

(*c*) Neutrons: $\beta < 1$. The variation in intensity of the TDS is much less pronounced than for (*a*) and (*b*). For a given value of q, the integrated intensity per mode is proportional to $1/q^2$. However, the number of modes participating in the scattering falls as the scattering surface approaches the reciprocal-lattice point, and the two effects combine to produce a flat TDS background near the Bragg peak. I_{TDS} is then zero.

In this paper we shall describe an experiment on silicon illustrating the sharp distinction between cases (*b*) and (*c*). The neutron Laue technique was used as this is a convenient method of determining I_{TDS} as a function of neutron wavelength.

2. Experiment

The single-crystal Laue method with neutrons was first proposed by Buras & Leciejewicz (1964). Polychromatic neutrons are scattered at a fixed angle 2θ by the sample and the time-of-flight technique is used to separate the detected neutrons in accordance with their wavelength. The time of flight, t, for neutrons of wavelength λ is related to the total length of the flight path, L, by

$$\lambda = 0{\cdot}003955\, t/L, \qquad (3)$$

where λ is in Å, t in μs and L in m. The timing measurement requires the initial production of neutron pulses, no more than a few μs in duration, which disperse themselves in time as they travel to the sample and are then scattered to the detector.

The neutron source for the present experiment was the Harwell electron linear accelerator Helios (Lynn, 1980) which was operated at a pulse repetition frequency of 75 Hz – sufficiently small to avoid frame overlap between successive pulses. A single crystal of dislocation-free silicon, in the form of a circular disc 50 mm in diameter and a few mm in thickness, was mounted on large goniometer arcs and placed on the ω-rotation table of the diffractometer which has a flight path, L, from the moderator to the detector

of 11.96 m. The arcs had been adjusted previously to bring the [220] axis, lying in the plane of the disc, into the horizontal plane. The [112] axis of the crystal was normal to this plane. The detector was set at a fixed angle 2θ in the range 20 to 60°, the [220] axis set at $90° - \theta$ to the incident beam, and intensity measurements carried out of the *hh*0 zone of reflections (see Fig. 2). The widths of the time channels chosen for the multi-channel analyser were 2 or 4 μs and the total time of counting at a given 2θ was four days.

Fig. 3 shows some typical data, illustrating the Bragg and thermal diffuse scattering associated with the 220 and 440 peaks. The TDS is particularly pronounced since its intensity is governed by the kinematic conditions of scattering, whereas the Bragg intensity for a perfect crystal is limited by dynamical diffraction and is independent of the thickness t of the crystal (apart from weak *Pendellösung* oscillations) for t exceeding the extinction distance. The background in Fig. 3 is flat at a sufficiently large distance from the peaks and is extrapolated as a broken line under the peaks.

The integrated intensity (Bragg+TDS) was measured above this broken line, and I_{TDS} was separated from the integrated Bragg intensity by estimating the latter from the longest-wavelength diffraction peaks where the TDS is known to be flat. The total integrated intensities for the *hh*0 reflections were measured at four different scattering angles. These results are analysed in the next section.

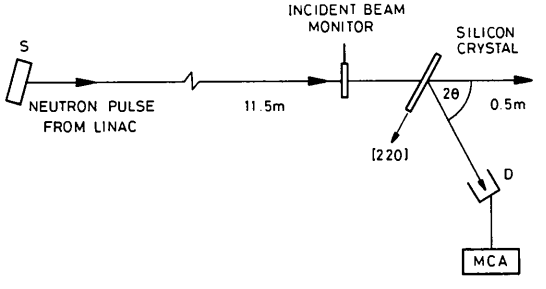

Fig. 2. Schematic arrangement of a pulsed neutron diffraction experiment. *S* represents the neutron source and associated moderator. *D* is the detector and MCA is the multi-channel time analyser.

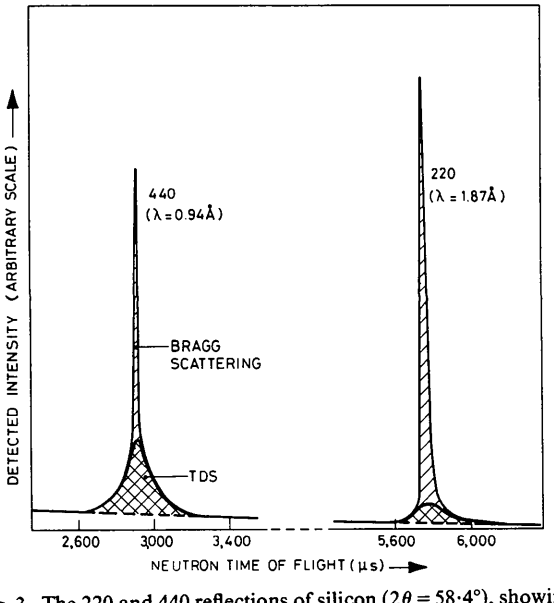

Fig. 3. The 220 and 440 reflections of silicon ($2\theta = 58{\cdot}4°$), showing TDS under the Bragg peak.

3. Analysis of experimental data

Firstly, we assume that the TDS under the Bragg peak arises entirely from one-phonon scattering. (Multi-phonon scattering will be largely subtracted in the background measurement.) Using the kinematic theory for the one-phonon scattering of neutrons of fixed wavelength λ, and making the somewhat drastic assumption that the volume scanned is a sphere centred on the reciprocal-lattice point, we find that the integrated intensity of one-phonon scattering I_{TDS}

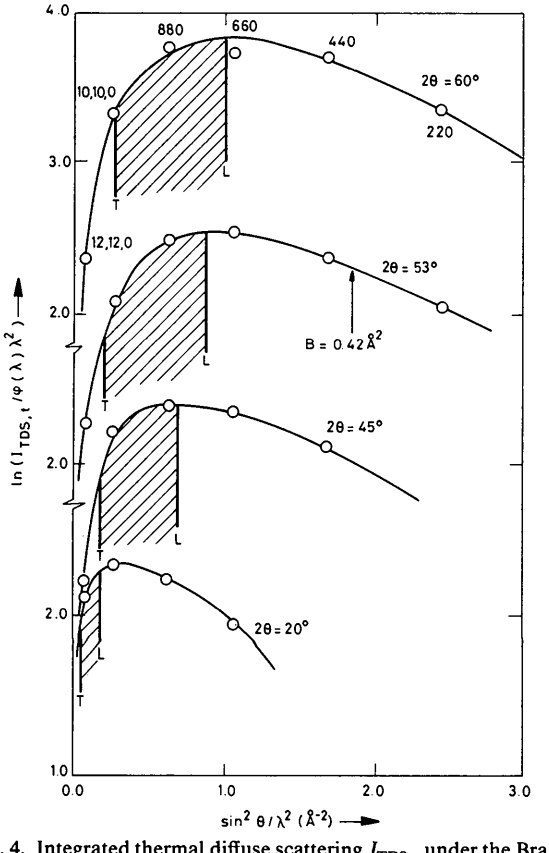

Fig. 4. Integrated thermal diffuse scattering $I_{TDS,t}$ under the Bragg peak divided by $\varphi(\lambda)\lambda^2$ *versus* $\sin^2\theta/\lambda^2$ at a series of scattering angles. The indices are given of the reflections that were measured along the [110] direction. $I_{TDS,t}$ falls off sharply when the neutron velocity drops below the velocity of sound in the crystal.

for faster-than-sound neutrons is (Willis & Pryor, 1975)

$$I_{\mathrm{TDS},\lambda} = \text{constant} \times (\sin^2\theta/\lambda^2) F^2 e^{-2M} k_B T. \quad (4)$$

Here F is the structure factor for Bragg scattering, e^{-2M} is the Debye-Waller factor (where $M = B\sin^2\theta/\lambda^2$) and T is the absolute temperature. The constant includes the elastic constants and the range of scan. Equation (4) is essentially unchanged for more realistic scans (Cooper, 1971).

Expression (4) is readily converted to the time-of-flight case by using the prescription of Buras & Gerward (1975). Thus

$$I_{\mathrm{TDS},t} = \text{constant} \times \varphi(\lambda)\lambda^2 F^2 e^{-2M} k_B T, \quad (5)$$

where $\varphi(\lambda)$ is the incident-beam intensity per unit wavelength range. If we plot

$$I_{\mathrm{TDS},t}/[\varphi(\lambda)\lambda^2 F^2 T]$$

on a logarithmic scale *versus* $\sin^2\theta/\lambda^2$, the points should lie on a straight line of slope $-2B$.

The measured data have been normalized to the incident flux $\varphi(\lambda)$, which was determined by monitoring the incident spectrum with a dilute ^{3}He detector and correcting for the variation of detector efficiency with neutron wavelength. Moreover, T is constant (293 K) and the structure factor F of silicon is the same for all reflections in the $hh0$ zone. Thus in Fig. 4 we have simply plotted $\ln(I_{\mathrm{TDS},t})/\varphi(\lambda)\lambda^2$ *versus* $\sin^2\theta/\lambda^2$.

At large values of $\sin^2\theta/\lambda^2$ the curves have a negative slope indicating $B \sim 0{\cdot}42$ Å^2, which is close to the accepted value, $B = 0{\cdot}46$ Å^2, quoted by Krec & Steiner (1984). However, as the wavelength increases and the neutron velocity falls below the velocity of sound in the crystal, there is a sharp fall-off in the integrated intensity I_{TDS} [as compared with that calculated from (5)]. The neutron velocity v is related to its wavelength by the de Broglie relation $\lambda = h/(m_n v)$. The lines L and T in Fig. 4 indicate the range of $\sin^2\theta/\lambda^2$ over which the neutron velocity lies between the maximum longitudinal (L) and minimum transverse (T) sound velocities. In the time-of-flight case the locus in reciprocal space for elastic scattering is a line along the reciprocal-lattice vector, unlike the fixed-wavelength case where this locus is the Ewald sphere. This line is at $90° - \theta$ to the scattered wave vector $\mathbf{k}$ and so a geometrical term, $\sec\theta$, is necessary in calculating the positions of L and T in Fig. 4. The sound velocities were calculated from the elastic constants given by McSkimin (1953).

The authors are especially grateful to Dr A. D. Taylor of the Rutherford Appleton Laboratory for his advice on shielding for the diffractometer. The computer programs used in the analysis were written by Mr A. S. Thornton and the silicon crystals were generously supplied by Mr N. W. Crick. We are also grateful for the expert help given us by the staff of the Helios linear accelerator and the Dido reactor at Harwell.

References

BURAS, B. & GERWARD, L. (1975). *Acta Cryst.* A31, 372-374.
BURAS, B. & LECIEJEWICZ, J. (1964). *Phys. Status Solidi*, 4, 349-355.
COOPER, M. J. (1971). *Acta Cryst.* A27, 148-157.
KREC, K. & STEINER, W. (1984). *Acta Cryst.* A40, 459-465.
LYNN, J. E. (1980). *Contemp. Phys.* 21, 483-500.
MCSKIMIN, H. J. (1953). *J. Appl. Phys.* 24, 988-997.
WILLIS, B. T. M. (1970). *Acta Cryst.* A26, 396-401.
WILLIS, B. T. M. & PRYOR, A. W. (1975). *Thermal Vibrations in Crystallography.* Cambridge Univ. Press.

Acta Cryst. (1986). A42, 191-197

The Intensity Fringes of Three Coupled Waves in Crystals

BY JOHANNES BREMER

Institutt for Røntgenteknikk, Universitetet i Trondheim-NTH, 7034 *Trondheim-NTH, Norway*

AND GUNNAR THORKILDSEN

Rogaland Distriktshøgskole, Ullandhaug, 4000 *Stavanger, Norway*

(*Received* 14 *August* 1985; *accepted* 26 *November* 1985)

Abstract

Two different kinds of interaction between three waves D_0, D_h and D_g in a perfect crystal are investigated in the case of Laue scattering using the Takagi-Taupin equations. Polarization effects (coupling between $\hat{\sigma}$ and $\hat{\pi}$ waves) are neglected, and it is assumed that the incoming vacuum wave $D_0^{(e)}$ has a small wave-front area whose spatial extension is simulated by a point source on the crystal surface. The solutions of the diffraction equations thus constitute the boundary-value Green functions for the wave

0108-7673/86/030191-07$01.50